Earth Systems and Environment (2019) 3:483–490
https://doi.org/10.1007/s41748-019-00113-0

ORIGINAL ARTICLE

Heat Balance in the Sharm Obhur and Exchange with the Red Sea

Badriah M. Alshreem[1] · Mohammed A. Alsaafani[1,2] · Turki M. Alraddadi[1] · Cheriyeri Poyil Abdulla[1]

Received: 1 June 2019 / Accepted: 12 August 2019 / Published online: 24 August 2019

Abstract

A comprehensive understanding of the balance and exchange of heat is vital to explore the interaction between atmosphere and ocean. Sharm Obhur is one of the most important lagoons along the eastern coast of the Red Sea. In situ observations of current speed and direction, temperature, and salinity along with near surface meteorological parameters are used to investigate monthly variability of heat balance in the Sharm Obhur and the exchange with the Red Sea. The net heat flux in the Sharm shows a notable seasonality with an annual heat loss of 49 W m^{-2}. The heat loss in the region peaked during December while maximum heat gain noticed during August. The entrance of the Sharm is well mixed during winter, while it is stratified by 2–3 °C during summer. Heat exchange between the Sharm and the Red Sea shows significant seasonality associated with the velocity of spring and neap flows. Interestingly, the annual net heat gain of 49.9 W m^{-2} noticed from the heat exchange is well compensated by the net surface heat loss of 49 W m^{-2}.

Keywords Net heat flux · Heat exchange · East Coast of the Red Sea · Air–sea interaction

1 Introduction

Sharm Obhur (here and after, Sharm) is one of the most important, lagoons along the eastern coast of the Red Sea, it is considered as a recreational coastal inlet of Jeddah city. The Sharm is about 10 km long and 0.5 km width with a maximum width of about 1.2 km, giving an approximate area of 5.6 km^2 (Alsaafani et al. 2017; Rasul and Stewart 2015). The depth decreases from 35 m at the entrance to about 6 m near the head (Basaham et al. 2006; Basaham and El-Shater 1994; Behairy et al. 1983). The temperature of the Sharm varied between 23.7 and 30.1 °C, while the salinity varied between 39.11 and 40.14 PSU during winter and late summer, respectively (El-Rayis and Eid 1997). Both temperature and salinity show a gradual increase towards the head of the Sharm (Ahmad and Sultan 1993; Alsaafani et al. 2017; Basaham et al. 2006). The tidal type in the Sharm is mixed semidiurnal (Shamji and Vineesh 2017), with very small tidal range about 0.3 m (Ahmad and Sultan 1993).

Most studies in the Sharm were concerning about the biological, geological, and chemical characteristics of the Sharm (Basaham et al. 2006; Basaham and El-Shater 1994; Behairy et al. 1983; Fahmy and Saad 2009; Farawati et al. 2008; Rasul et al. 2009). There have been several studies in the literature describing the exchange of water between the Sharm and the Red Sea and describing the hydrographical condition of the area. For example, Al-subhi (2010), Albarakati (2009), Alsaafani et al. (2017), and El-Rayis and Eid (1997) described the general form of hydrographic structure and water balance of the Sharm. They found three water masses at the entrance of the Sharm which indicates two layers system: an inflow of the surface (high salinity) and intermediate (low salinity) water masses, and outflow of the deep-water mass with high salinity. Albarakati (2009) described the vertical hydrographic structure of the Sharm, which is almost mixed during the winter and stratified during the summer.

The flow at the entrance shows two layers with surface inflow (low salinity) and deep outflow (high salinity). While Al-subhi (2010) based on observations for 2 months during 2010 stated that the water column is well mixed during the summer, and the variation of current speed was between 26.4 and 82.9 cm s^{-1} with the highest magnitude during October. A more comprehensive study to describe the seasonal changes of the hydrographic structure of the Sharm

✉ Badriah M. Alshreem
bshreem@stu.kau.edu.sa

1 Department of Marine Physics, Faculty of Marine Sciences, King Abdulaziz University, Jeddah, Saudi Arabia

2 Department of Earth and Environmental Sciences, Faculty of Science, Sana'a University, Sana'a, Yemen

was conducted by Alsaafani et al. (2017). The study covered 10 months (2015–2016) based on nine field trips. Their results also confirm the previous findings of the two-layer structure in the Sharm: surface layer with low salinity and a deep layer with high salinity. They found maximum temperature as 33.22 °C during August and maximum salinity as 40.36 PSU during April, while minimum temperature and salinity reported during January as 25.05 °C and 38.97 PSU, respectively.

The estimation of the rate of exchange and the flushing time of the Sharm show considerable variability. El-Rayis and Eid (1997) estimated the flushing time between 1 and 4 days, while Albarakati (2009) estimated the flushing time as about 12 days. Recently, Alsaafani et al. (2017) show an average flushing time of the Sharm as 9.5 days.

The study of the heat and freshwater budget considered as one of the most important elements for understanding the interactions and exchanges between the ocean and atmosphere. The Red Sea circulation is thought to be driven by the surface buoyancy fluxes due to the heat and freshwater between the atmosphere and Ocean. Since it is one of the enclosed seas, the outflow of Red Sea water is warm and highly saline (Abdulla et al. 2018), and plays an important role in the circulation of the Gulf of Aden and the Arabian Sea (Abdulla et al. 2016, 2019; Sofianos et al. 2002). The exchange of heat and freshwater between the Red Sea and Gulf of Aden via the Bab al-Mandab Strait was estimated based on observations of water characteristics and current velocity at the entrance (Alsaafani and Shenoi 2004; Murray and Johns 1997; Sofianos et al. 2002).

The Sharm represents a typical model for the Red Sea in terms of the shape and oceanographic conditions, and hence understanding its dynamics would help further in thoughtful the entire Red Sea. Despite the importance of the Sharm, there is no previous study on the heat budget of the Sharm and the heat exchange with the Red Sea. The objectives of this study are to estimate the heat balance of the Sharm and heat exchange with the Red Sea, by analyzing a 1-year record of the hydrographic data and current profiles aligned with meteorological data. The following sections of this paper are organized as follows: Sect. 2 describes the data used and analyzing methodology, Sect. 3 describes results and discussion, and the last section is for the conclusion.

2 Materials and Methods

2.1 Data Sets Used

The present study relied on 19 field trips to measure the temperature in the Sharm to calculate the heat and freshwater from April 2015 to March 2016 (for 12 months). The field trips were conducted during the following seasons: five trips during summer (June–September), seven trips during winter (December–March), three trips during spring (April–May), and four trips during fall (October–November). Out of the eight stations in each trip, the hydrographic profile positioned near the entrance of the Sharm with the Red Sea (21.7547°N, 39.1300°E) is selected to estimate the heat exchange (Fig. 1). An ACTD-RS instrument was set to measure the temperature and the salinity vertical profiles.

The hydrographic data have been collected for every 5 m interval starting from 0.5 m at sea surface up to 25 m deep. The temperature for August and September was missing due to a technical fault at this station, which is solved for the month of August by taking profiles from nearest station (less than 2 km away) and for the month of September by interpolating from the previous and following months.

The second data source for this study is the Acoustic Doppler Current Profiler (ADCP) data, which was deployed near the entrance of the Sharm at the hydrographic station 2 (Fig. 1). The instrument gives current velocity at every 15 min for the entire water column giving ten cells each of 3 m from the surface to the bottom, for the same period of the hydrographic data. The daily mean was estimated by smoothening and filtering the 15 min ADCP data following Alsaafani et al. (2017) and Godin (1972) using $\frac{\alpha_{24}^2 \cdot \alpha_{25}}{24^2 \cdot 25}$. This filter application requires 71 consecutive observations. A sequence of means is first computed for 25 observations,

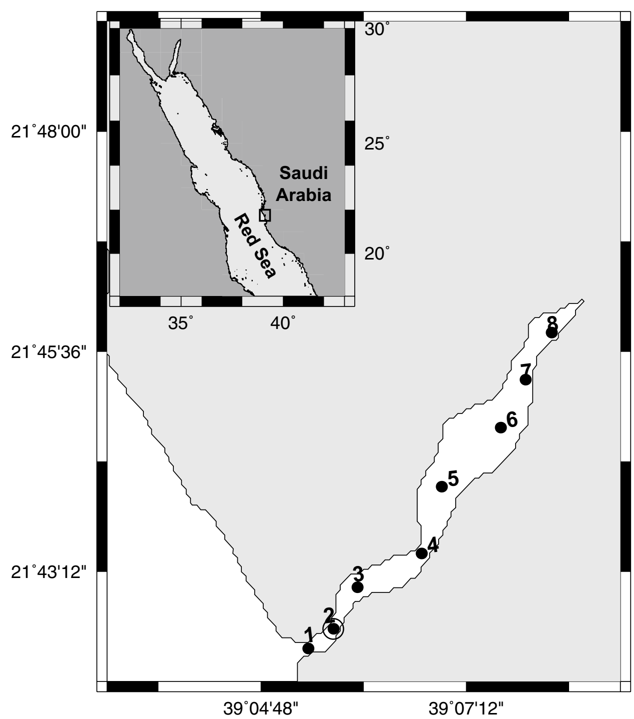

Fig. 1 Map of the study area, the black dots show the location of the hydrographic stations, while the circle shows the location of the ADCP

followed by a series of means for 24 of these means and finally the sum of this last series which gives the daily mean.

The third source of data was the daily meteorological data obtained from General Authority of Meteorology and Environmental Protection (GAMEP), the data include relative humidity (RH), wind speed (WS), air temperature (Ta), and air pressure (P). Unfortunately, the short-wave radiation was not available from the GAMEP, so the monthly short-wave radiation (Qs) from TropFlux data were used in this study (Kumar et al. 2012). The monthly average of meteorological parameters for the study period is listed in Table 1.

2.2 Methods

2.2.1 Estimation of Heat Balance in the Sharm

The heat balance was estimated based on the following equation (Ahmad and Albarakati 2015):

$$Q_s - Q_{lw} \mp Q_h - Q_e = Q_A, \tag{1}$$

where Q_s is the short-wave radiation, Q_{lw} is the net long-wave radiation outward the sea surface, Q_h is the sensible heat flux carried by conduction, Q_e is the latent heat flux carried by evaporation, and Q_A is the net horizontal advection.

2.2.1.1 Net Long-Wave Radiation (Q_{lw}) The net long-wave radiation was estimated by the following (Ahmad and Albarakati 2015):

$$Q_{lw} = Q_{lwo}(1 - cn^2) + 4\varepsilon\sigma(\mathrm{SST})^3(\mathrm{SST} - T_{air}) \tag{2}$$

$$Q_{lwo} = \varepsilon\sigma(\mathrm{SST})^4\left(a - b\sqrt{e_a}\right), \tag{3}$$

where ε is the average coefficient of emissivity at the sea surface, with a value of 0.985 (Kraus 1972), σ is the Stefan–Boltzmann constant (5.67×10^{-8} W m^{-2} K^{-4}), a, b are constants (0.39, 0.05 respectively), cn is the cloud cover for Jeddah as a monthly average, and e_a is vapor pressure.

2.2.1.2 Sensible Heat Flux (Q_h) The sensible heat flux (Q_h) was estimated using the bulk formula method (Ahmad et al. 1989; Sultan and Ahmad 1997; Sultan and Elghribi 2003):

$$Q_h = \rho_a c_p c_h(\mathrm{SST} - T_{air})W_s\,, \tag{4}$$

where SST–T_{air} is the sea–air temperature difference in Kelvin, the density of the air $\rho_a = 1.2$ kg m^{-3}, c_p is specific heat of air at constant pressure, W_s is the wind speed, and c_h is the sensible heat coefficient. Following Ahmad et al. (1989), the value of c_h is 1.7×10^{-3}, given by the following:

$$Q_h = 2.14(\mathrm{SST} - T_{air})W_s\,. \tag{5}$$

2.2.1.3 Latent Heat Flux (Q_e) The latent heat flux (Q_e) was estimated using the bulk formula method (Ahmad et al. 1989; Sultan and Ahmad 1997):

$$Q_e = \rho_a L c_e(q_s - q_a)W_s, \tag{6}$$

where $c_e = 1.7 \times 10^{-3}$ is the latent heat flux coefficients following Ahmad et al. (1989), q_a is the specific humidity at atmosphere, q_s is the saturated specific humidity at sea surface, and L is the latent heat of evaporation (2.45×10^6 J kg^{-1}). Giving the Q_e as

$$Q_e = 3.12(e_s - e_a)W_s, \tag{7}$$

where e_s and e_a are saturated and actual vapor pressure, respectively.

2.2.2 Estimation of Advective Heat Flux (Q_A)

To estimate the heat exchange between the Sharm and the Red Sea through the entrance, the following equation was used (Ahmad and Albarakati 2015; Tragou et al. 1999):

$$Q_A = \frac{1}{A}C_{pw}[(V_i T_i - V_o T_o) - AE_{net}\mathrm{SST}], \tag{8}$$

Table 1 Monthly values of meteorological parameters

Years	Months	WS (m s^{-1})	SST (°C)	Cloud cover	T_{air} (°C)	RH (%)	P (hPa)
2015	April	2.69	27.08	0.04	28.98	49.77	1011.27
	May	2.69	28.58	0.17	30.88	53.69	1009.02
	June	2.69	29.21	0.19	30.84	53.72	1007.20
	July	2.72	30.26	0.11	32.79	48.26	1006.15
	August	2.71	31.31	0.37	33.88	61.39	1005.06
	September	2.46	32.64	0.26	32.95	60.49	1007.68
	October	2.34	31.79	0.23	31.77	57.79	1011.34
	November	2.44	30.19	0.07	28.78	56.44	1013.15
	December	2.86	28.28	0.33	25.07	48.31	1017.62
2016	January	2.70	25.91	0.28	23.95	52.11	1017.65
	February	2.68	26.65	0.23	25.29	51.42	1016.25
	March	3.17	26.43	0.29	27.38	57.43	1012.19

where A is the area of the Sharm 5.6×10^6 m^2 (Alsaafani et al. 2017), V_i and V_o are mean volume fluxes, ρ is the density of water, E_{net} is the difference between evaporation and precipitation, and C_{pw} is specific heat of sea water.

3 Results and Discussion

3.1 Seasonal Variability of Atmospheric Parameters and Surface Temperature

The monthly mean variations of wind speed (W_s), air temperature (T_{air}), relative humidity (RH), cloud cover, pressure (P), and sea surface temperature (SST) in the area of the Sharm for a 1-year period from April 2015 to March 2016 are reported in Table 1 and shown in Fig. 1. In general, the SST shows the annual cycle clearly, where it increases steadily from April (27.08 °C) to reach maximum value in September (32.64 °C), and then decreases gradually towards the winter season with a minimum value of 25.91 °C in January. The air temperature (T_{air}) shows a similar pattern, increasing from April with a value of 28.98 °C to reach a maximum value of 33.88 °C in August, and then, it decreases toward the winter season with a minimum value of 23.95 °C in January.

It is appearing that the seasonal variability of SST is following the same pattern of the T_{air} where it decreases during the fall and winter seasons. Statically, there is a strong positive correlation between SST and T_{air} with a value of 0.83.

Figure 2b shows the wind speed viability over the study period. No significant variation is observed in the wind speed values during the summer and spring seasons. The peak of wind speed occurs in March (winter season) with a value of 3.17 m s^{-1} and the lowest occurs in October (fall season) with a value of 2.34 m s^{-1}. Many researchers have shown that there is a negative relationship between SST and wind speed (Bjerknes 1964; Huang and Qiao 2009; Hurrell 1995; Shukla and Misra 1977), so the statistical analysis between them show a negative relation between SST and wind speed with a correlation value of -0.64. Figure 2c shows that the sea level pressure decreases to a minimum value of 1005.06 hPa) in summer season (August), which later increases to maximum value of 1017.65 hPa in the winter season (January).

Figure 2d shows that the relative humidity decreases during winter season to a minimum value of 48.31% in December and increases during summer to reach the maximum value of 61.39% in August, which clearly shows the annual cycle. During July, the relative humidity drops to a minimum value of 48.26%, which may be due to low cloud cover. In general, the cloud cover is low all over the year, with some increase to a maximum in August, and then, it decreases to a minimum in November (Fig. 2e).

3.2 Seasonal Variability of Surface Heat Fluxes

The monthly variability of surface heat fluxes (radiative and turbulent) in the Sharm is shown in Fig. 3 and listed in Table 2. The highest incoming short-wave radiation (Q_s) was found from April to July with about 250 W m^{-2}, while the minimum was observed in December with a value of 133 W m^{-2}. It is evident that there is a drop in Q_s in August with a value of 225 W m^{-2}, which might be related to the sudden increase in cloud coverage in the same month (Fig. 2). The seasonal averages of Q_s for the winter, spring, summer, and fall seasons are, respectively, 170 W m^{-2}, 252 W m^{-2}, 235 W m^{-2}, and 183 W m^{-2}. Annual average Q_s for the Sharm is 207.33 W m^{-2} with a range of 120 W m^{-2}. The net outgoing long-wave radiation (Q_{lw}) is high during the winter with maximum value in December (101 W m^{-2}), and then, it decreases to reach the minimum during August (28 W m^{-2}). The SST–T_{air} variations are positive during winter and negative during summer causing seasonal variability in the Q_s with a range of 73 W m^{-2}, and an annual average of 66 W m^{-2}.

The maximum of latent heat flux (Q_e) observed in December (206 W m^{-2}), while minimum in August (112 W m^{-2}) with annual average 147 W m^{-2}. As seen in the previous section that, the SST are warmer compared to T_{air} over the Sharm for the month of November–February, while it is reverse for the rest of the months. Q_e show similar variability to that of SST–T_{air}, where the highest Q_e occurs during the winter season (November–February), while it decreases during the summer season to the minimum value in August (112 W m^{-2}). We noticed a sudden increase in Q_e during July which might be attributed to the decrease in relative humidity.

Similarly, the Q_h variations are well matching with SST–T_{air} variations, where its negative from March to September, with the minimum values during July–August (~ -15 W m^{-2}). From September, the Q_h start increasing reaching its maximum value of about 20 W m^{-2} in December.

The monthly surface net heat flux (Q_{net}) shows that there is heat loss during winter months with maximum value -193 W m^{-2} in December, while heat gain is observed during the rest of the year with maximum value 99 W m^{-2} in August (Table 2). The annual mean of Q_{net} shows a surface heat loss with a value of -49 W m^{-2}.

3.3 Heat Exchange with the Red Sea

Advection of heat is one of the main components of the heat budget in the ocean. To estimate the adverted heat between the Sharm and the Red Sea, ADCP mooring was deployed for 1 year at the entrance to estimate along entrance flow from the surface to the bottom. Monthly temperature profiles

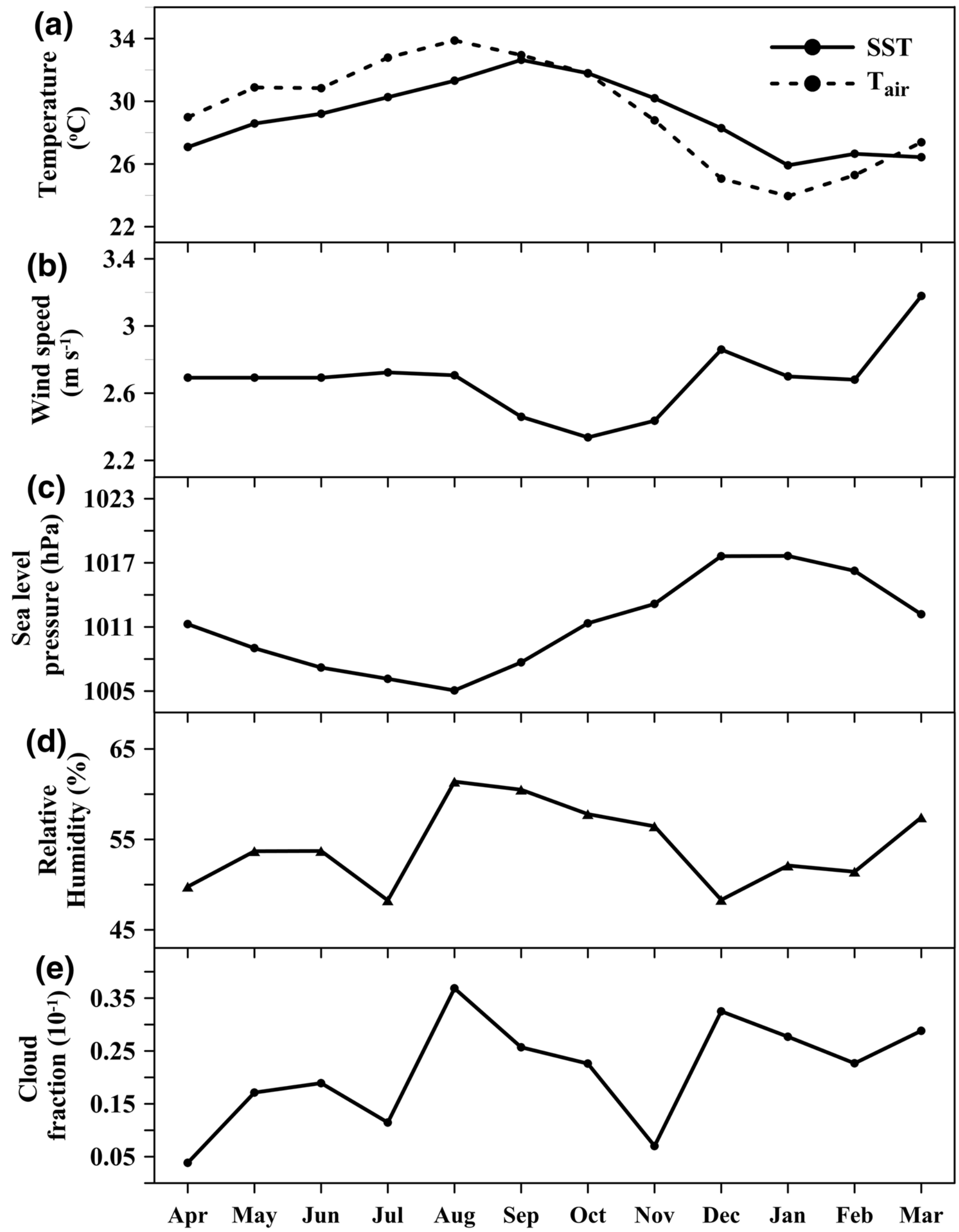

Fig. 2 Monthly variation of meteorological parameters

were also collected at the same location for the same period. Both data sets were used to estimate the heat exchange between the Sharm and the Red Sea.

Figure 4 shows monthly variability of vertical profiles of temperature. At the surface, it increases from 26 °C during February to the maximum of 32–33 °C during August–September. The temperature section shows vertical mixed water column from the surface to the maximum depth (30 m) during winter from November to February. From April to October at the top 15 m, the vertical temperature increases gradually to reach a maximum difference of 2–3 °C (August and September) between the surface and deep layers. The vertical structure of temperature during June and October shows a similar structure to that reported by Al-subhi (2010) near the entrance.

The vertical velocity structure along the entrance is shown in Fig. 5, which shows clearly a two-layer structure with the surface inflow of about 15 m depth and deep outflow. The speed of the bottom layer is higher than that of the surface, which is normal for compensating the reduction of the entrance width (V-shape). The signal of the spring and neap flow is clearly seen in the alternating of the strength and weakening of the flow for both layers. The two-layer structure of the flow at the entrance of the Sharm was reported in the previous studies (Albarakati 2009; Alsaafani et al. 2017; El-Rayis and Eid 1997).

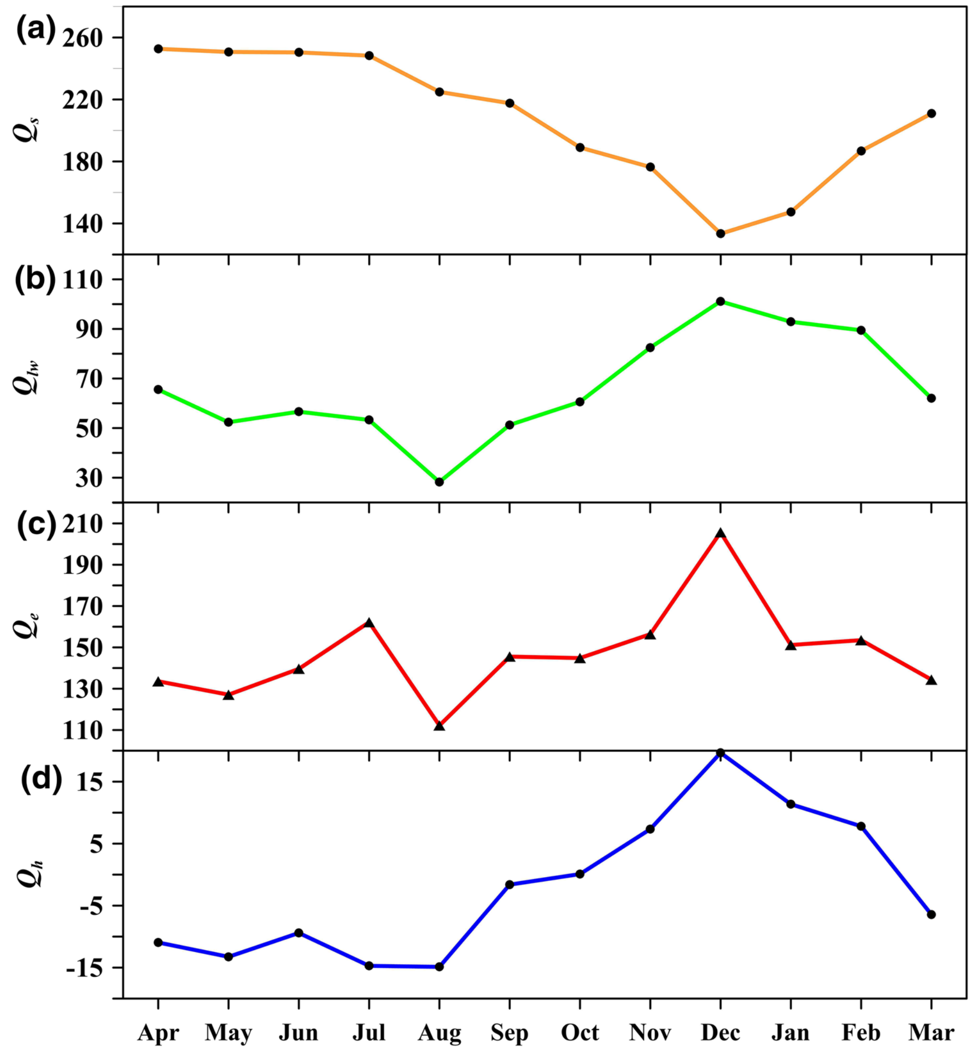

Fig. 3 The seasonal variability of surface heat flux components in the Obhur region

Table 2 The monthly mean values of surface heat flux components in W m^{-2}

Months	Q_s	Q_{lw}	Q_e	Q_h	Q_{net}
Apr	253	66	134	− 11	65
May	251	52	127	− 13	84
Jun	250	57	140	− 9	64
Jul	248	53	162	− 15	48
Aug	225	28	112	− 15	99
Sep	218	51	146	− 2	22
Oct	189	61	145	0	− 17
Nov	176	82	156	7	− 70
Dec	133	101	206	20	− 193
Jan	147	93	151	11	− 108
Feb	187	89	154	8	− 64
Mar	211	62	134	− 6	21
Annual mean of the Q_{net}					− 49

For the first time, the monthly values of the heat advection between the Sharm and the Red Sea are estimated using Eq. (8). Figure 6 shows the variability of heat exchange, where relatively large month-to-month variability is clearly visible. This variability is due to the change in along entrance velocity of spring and neap flows. As expected, heat gain during the summer months and loss during the winter months are evident (Fig. 6). In general, the annual mean of heat exchange compensates for the annual mean of the net heat flux at the surface with heat gain of 49.9 W m^{-2} compared with the surface heat loss of 49 W m^{-2}.

4 Conclusion

In this study, a 1-year long record of surface meteorological data, current, and temperature have been used to estimate the monthly heat fluxes and heat balance in the Sharm of Obhur. The result shows that there is heat loss during winter (maximum loss in December, − 193 W m^{-2}) and heat gain

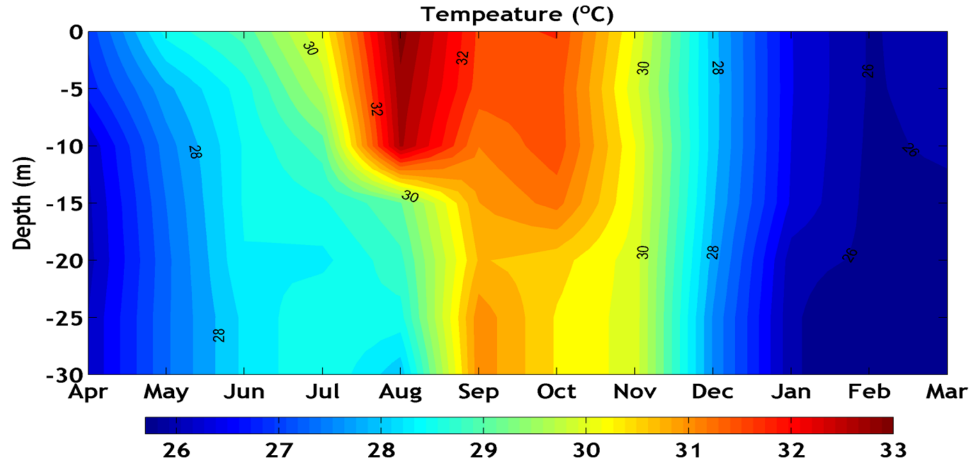

Fig. 4 Monthly variation of vertical temperature profiles near the entrance

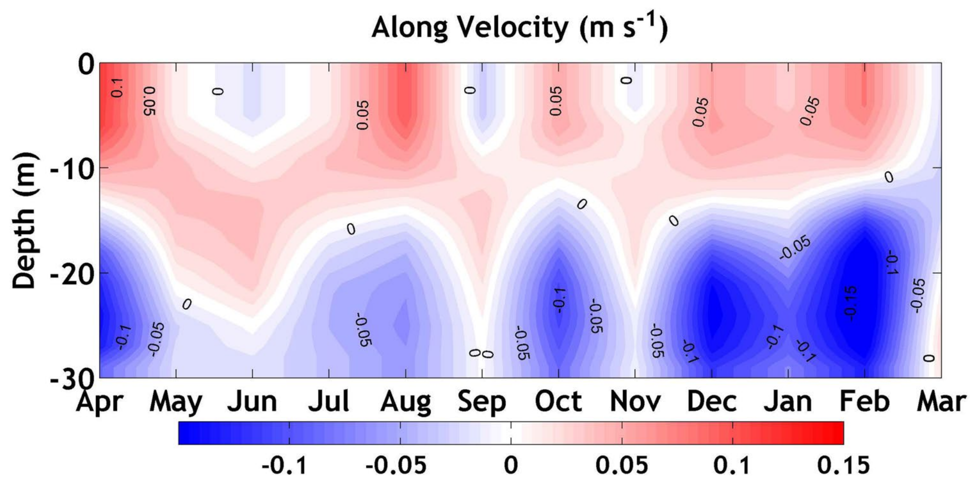

Fig. 5 Monthly variation of current along the entrance

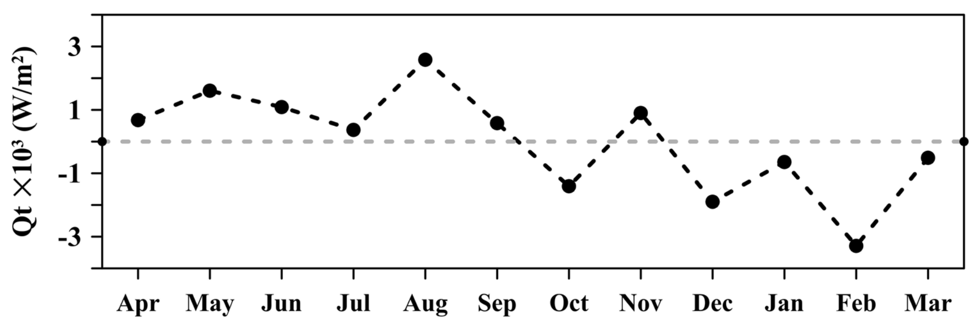

Fig. 6 Monthly variation of heat exchange through the entrance

during summer (maximum gain in August, 99 W m^{-2}) with an annual surface heat loss of -49 W m^{-2}.

This paper has clearly shown that the vertical temperature structure at the entrance of the Sharm is well mixed during the winter (similar to the structure reported by Al-subhi 2010), while the temperature structure is stratified during the summer with a maximum difference between the two layers of 2–3 °C. The vertical velocity structure at the Sharm shows clearly a surface inflow from the Red Sea to the Sharm and subsurface outflow from the Sharm to the Red Sea. The magnitude of the subsurface layer velocity is higher than that at the surface due to the shape of the entrance. The two-layer structure shown in this study is consistent with those reported by previous studies (Albarakati 2009; Alsaafani et al. 2017; El-Rayis and Eid 1997).

One of the more important findings from this study is the estimation of the heat advection between the Sharm and the Red Sea, which shows a significant variability from month to month. This variability is due to the relatively strong variation of velocity (spring and neap flows) at the entrance. Annual mean heat advection shows a heat gain of 49.9 W m^{-2}, while the annual mean net heat flux resulted in a heat loss of − 49 W m^{-2}. It is interesting to note that the observed annual surface heat loss (− 49 W m^{-2}) compensates the excess in annual net heat advection (49.9 W m^{-2}).

Acknowledgements The authors appreciate the time and efforts of Mr. Shanas P.R., Mr. S. Garbi, Mr. A. Taqi, Mr. Kamalaldien M., and Mr. A. Alamshani in data collection. The authors also acknowledge the Presidency of Meteorology and Environment (PME) for providing the meteorological data. The author BMA acknowledges the Deanship of Graduate Studies, King Abdulaziz University, Jeddah, for providing an MSc fellowship.

Compliance with ethical standards

Conflict of interest We wish to confirm that there are no known conflicts of interest associated with this publication and there has been no significant financial support for this work that could have influenced its outcome.

References

Abdulla CP, Alsaafani MA, Alraddadi TM, Albarakati AM (2016) Estimation of mixed layer depth in the Gulf of Aden: a new approach. PLoS One 11:e0165136. https://doi.org/10.1371/journal.pone.0165136

Abdulla CP, Alsaafani MA, Alraddadi TM, Albarakati AM (2018) Mixed layer depth variability in the Red Sea. Ocean Sci 14(4):563–573. https://doi.org/10.5194/os-14-563-2018

Abdulla CP, Alsaafani MA, Alraddadi TM, Albarakati AM (2019) Climatology of mixed layer depth in the Gulf of Aden derived from in situ temperature profiles. J Oceanogr 75:335. https://doi.org/10.1007/s10872-019-00506-9

Ahmad F, Albarakati AMA (2015) Heat balance of the Red Sea. In: Rasul N, Stewart I (eds) The Red Sea. Springer earth system sciences. Springer, Berlin, Heidelberg

Ahmad F, Sultan SAR (1993) Tidal and sea level changes at Jeddah, Red Sea. Pak J Mar Sci 2(2):77–84

Ahmad F, Sultan SAR, Moammar MO (1989) Monthly variations of net heat flux at the air–sea interface in coastal waters near Jeddah, Red Sea. Atmos Ocean 27(2):406–413. https://doi.org/10.1080/07055900.1989.9649343

Albarakati AMA (2009) Water exchange of Sharm Obhur, Jeddah, Red Sea. JKAU Mar Sci 20(1):49–58. https://doi.org/10.4197/Mar.20-1.4

Alsaafani MA, Shenoi SSC (2004) Seasonal cycle of hydrography in the Bab el Mandab region, southern Red Sea. J Earth Syst Sci 113(3):269–280. https://doi.org/10.1007/BF02716725

Alsaafani MA, Alraddadi TM, Albarakati AM (2017) Seasonal variability of hydrographic structure in Sharm Obhur and water exchange with the Red Sea. Arab J Geosci. https://doi.org/10.1007/s12517-017-3108-8

Al-subhi AM (2010) A study of vertical mixing processes in Sharm Obhur, Eastern Red Sea during summer. JKAU Mar Sci 22(1):97–111

Basaham AS, El-Shater A (1994) Textural and mineralogical characteristics of the surficial sediments of Sharm Obhur, Red Sea Coast of Saudi Arabia. JKAU Mar Sci 5(1):51–71. https://doi.org/10.4197/mar.5-1.5

Basaham A, Rifat A, El-Sayed M, Rasool N (2006) Sharm Obhur: environmental consequences of 20 years of uncontrolled coastal urbanization. JKAU Mar Sci 17(1):129–152. https://doi.org/10.4197/mar.17-1.8

Behairy AK, El-Rayis O, Ibrahim A (1983) Preliminary investigation of some heavy metals in water, sediments and plankton in Obhur Creek (Eastern Red Sea). JKAU Mar Sci 3:129–140

Bjerknes J (1964) Atlantic air–sea interaction. Advances in geophysics, vol 10. Elsevier, Amsterdam, pp 1–82

El-Rayis OA, Eid FM (1997) Hydrography and water budget of Obhur Creek, Red Sea. JKAU Mar Sci 8:29–45

Fahmy M, Saad M (2009) Temporal and spatial distribution of heavy metals in Obhur Creek, a coastal Red Sea water body north of Jeddah. J King Abdulaziz Univ Mar Sci 7(1):75–83. https://doi.org/10.4197/mar.7-1.8

Farawati R, AlMaradni A, Basaham A, El Sayed MA (2008) Reclaimed municipal wastewater used for the irrigation of green areas in Jeddah: 1—chemical characteristics. JKAU Mar Sci 19:121–146

Godin G (1972) The analysis of tides. University of Toronto Press, Toronto

Huang C, Qiao F (2009) The relationship between sea surface temperature anomaly and wind energy input in the Pacific Ocean. Prog Nat Sci 19(10):1409–1412

Hurrell JW (1995) Decadal trends in the North Atlantic Oscillation: regional temperatures and precipitation. Science 269(5224):676–679

Kraus EB (1972) Atmosphere–ocean interaction. Oxford University Press, London

Kumar BP, Vialard J, Lengaigne M, Murty VSN, Mcphaden MJ (2012) TropFlux: air–sea fluxes for the global tropical oceans—description and evaluation. Clim Dyn 38:1521–1543. https://doi.org/10.1007/s00382-011-1115-0

Murray S, Johns W (1997) Direct observations of seasonal exchange through the Bab el Mandab Strait. Geophys Res Lett 24(21):2557–2560

Rasul MA, Stewart C (2015) The Red Sea. The formation, morphology, oceanography and environment of a young ocean basin. J Near East Stud. https://doi.org/10.1086/371522

Rasul N, Al-Nomani S, Al-Hazmi O, Widinly N, Qutub A, Bantan R (2009) Bathymetric survey in Sharm Obhur. Springer, Berlin

Shamji VR, Vineesh TC (2017) Shallow-water tidal analysis at Sharm Obhur, Jeddah, Red Sea. Arab J Geosci 10(3):61. https://doi.org/10.1007/s12517-016-2822-y

Shukla J, Misra BM (1977) Relationships between sea surface temperature and wind speed over the central Arabian Sea, and monsoon rainfall over India. Mon Weather Rev 105(8):998–1002

Sofianos SS, Johns WE, Murray SP (2002) Heat and freshwater budgets in the Red Sea from direct observations at Bab el Mandeb. Deep-Sea Res Part II Top Stud Oceanogr 49(7–8):1323–1340. https://doi.org/10.1016/S0967-0645(01)00164-3

Sultan S, Ahmad F (1997) Heat budget of the Gulf of Aden: surface, advective and upwelling heat fluxes. Oceanol Acta 20(5):665–672

Sultan S, Elghribi N (2003) Sea level changes in the central part of the Red Sea. Indian J Mar Sci 32(June):114–122

Tragou E, Garrett C, Outerbridge R, Gilman C (1999) The heat and freshwater budgets of the Red Sea. J Phys Oceanogr 29(10):2504–2522. https://doi.org/10.1175/1520-0485(1999)029%3c2504:THAFBO%3e2.0.CO;2